

Characterization of a High-Gain Harmonic-Generation Free-Electron Laser at Saturation

A. Doyuran,¹ M. Babzien,¹ T. Shaftan,¹ L. H. Yu,¹ L. F. DiMauro,¹ I. Ben-Zvi,¹ S. G. Biedron,² W. Graves,¹ E. Johnson,¹ S. Krinsky,¹ R. Malone,¹ I. Pogorelsky,¹ J. Skaritka,¹ G. Rakowsky,¹ X. J. Wang,¹ M. Woodle,¹ V. Yakimenko,¹ J. Jagger,² V. Sajaev,² and I. Vasserman²

¹Brookhaven National Laboratory, Upton, New York 11973

²Advanced Photon Source, Argonne National Laboratory, Argonne, Illinois 60439

(Received 18 January 2001)

We report on an experimental investigation characterizing the output of a high-gain harmonic-generation (HGFG) free-electron laser (FEL) at saturation. A seed CO₂ laser at a wavelength of 10.6 μm was used to generate amplified FEL output at 5.3 μm . Measurement of the frequency spectrum, pulse duration, and correlation length of the 5.3 μm output verified that the light is longitudinally coherent. Investigation of the electron energy distribution and output harmonic energies provides evidence for saturated HGFG FEL operation.

DOI: 10.1103/PhysRevLett.86.5902

PACS numbers: 41.60.Cr

There is great interest in utilizing a high-gain single-pass free-electron laser (FEL) to generate high intensity, short pulse radiation in the spectral region from the deep ultraviolet down to hard x-ray wavelengths [1,2]. One approach, which has been the subject of widespread theoretical and experimental investigation [3–12], is called self-amplified spontaneous emission (SASE). In the SASE process, the spontaneous radiation emitted by quivering electrons near the beginning of a long undulator magnet is subsequently amplified as it copropagates with the electron beam through the magnet structure. A SASE FEL can produce short wavelength light with high peak power and excellent spatial mode. However, the light has poor temporal coherence (coherence time much shorter than the pulse duration) and chaotic shot-to-shot variations since the process is initiated through shot noise.

Recently, an alternate single-pass FEL approach utilizing a high-gain harmonic-generation (HGFG) scheme, which is capable of producing longitudinally coherent pulses, was demonstrated [13–16]. In a HGFG FEL the light output is derived from a coherent subharmonic seed pulse. Consequently, the optical properties of the HGFG FEL is a map of the characteristics of the high-quality seed laser. This has the benefit of providing light with a high degree of stability and control of the central wavelength, bandwidth, energy, and pulse duration which is absent from a SASE source. Furthermore, the HGFG source can produce light pulses with durations much shorter than the electron bunch length by synchronizing an ultrashort laser pulse to the electron beam. In this Letter we show through a series of measurements that the output of a HGFG FEL is saturated and longitudinally coherent. The experiments give good agreement with values obtained from theoretical simulations [17].

The experiments [15,16] were performed at the Accelerator Test Facility (ATF) at Brookhaven National Laboratory in collaboration with the Advanced Photon Source at Argonne National Laboratory. The principle of the HGFG

FEL was influenced by earlier work in the field [18–22], but differs from previous approaches in that the harmonic radiation is exponentially amplified. The experimental layout is illustrated in Fig. 1. A coherent 200 ps long, 10.6 μm seed pulse from a CO₂ laser interacts with the 6 ps long electron beam resonantly in the first (modulator) undulator. The seed light has a Rayleigh range of 0.8 m and a half-intensity beam diameter of 1.7 mm. The resulting energy modulation is then converted to a spatial bunching while the electron beam traverses a dispersion section (a three-dipole chicane). In the second (radiator) undulator, tuned to be resonant at 5.3 μm , the microbunched electron beam first emits coherent radiation and then amplifies it exponentially until saturation is achieved. First lasing of an HGFG FEL was reported in Refs. [15,16]. The HGFG pulse energy was measured to be $\sim 10^7$ times larger than the spontaneous radiation and 10^6 times larger than the SASE signal, which, in the case of the HGFG experiment, provides a background noise. The single shot spectral distribution of the HGFG output in the neighborhood of 5.3 μm was recorded by placing a thermal imaging camera at the exit plane of a monochromator. The full-width half-maximum (FWHM) bandwidth of the HGFG output was found to be 15 nm [16], much narrower than the SASE bandwidth. In this paper, we extend the earlier work by using a second-harmonic autocorrelator to measure the intensity pulse duration, and an interferometer to measure the coherence length. The agreement of these two measurements indicates excellent longitudinal coherence.

Numerical simulation [17] employing parameters similar to the current experiment was carried out using a modified version of the three-dimensional axis-symmetric code [14]. In this model, the radiation process is simulated using the Maxwell equations coupled to the classical equations describing the electron motion. A Monte Carlo method provides a random distribution of the initial conditions. Our model assumes that slippage effects are negligible

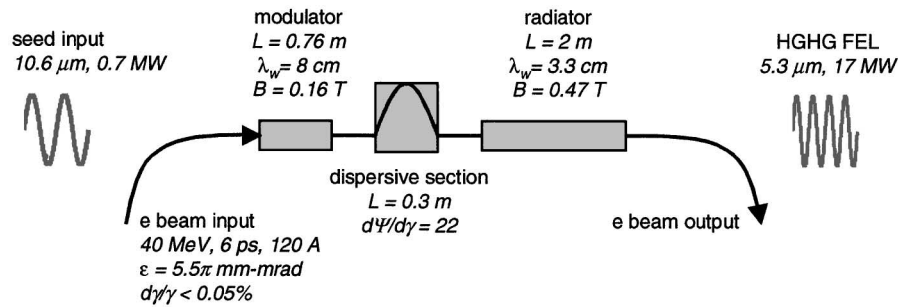


FIG. 1. HGHG experimental schematic and typical parameters. The LINAC produces 6 ps, 40 MeV electron pulses with a peak current of 120 A, emittance (ϵ), and energy spread ($d\gamma/\gamma$). Listed are the length (L), period (λ_w), and magnetic field (B) for the modulator and radiator. The dispersive section is 0.3 m long with a dispersion of $d\Psi/d\gamma$.

since the electron bunch length (6 ps) is longer than the slippage distance (1 ps).

In the HGHG process, energy modulation of the electron beam is generated in two ways: through the initial interaction of the seed laser with the electron beam in the modulator and through the HGHG FEL interaction in the radiator. The energy modulation produced in the radiator dominates. The amount of modulation is measured using an electron energy spectrometer after the radiator section. Because of the dispersion of the bending magnet downstream of the HGHG radiator undulator, the electrons with different energies will follow different trajectories. By adjusting the quadrupole strength to minimize the betatron motion in the horizontal direction, one can correlate the electron's position with energy and thus measure the energy distribution.

The electron beam energy distributions at the spectrometer with the CO₂ laser on (solid line) and with the CO₂ laser off (dashed line) are shown in Fig. 2. The effect of the CO₂ laser on the electron beam is dramatic, producing an energy modulation of $\Delta\gamma/\gamma = 2.5\%$. Using conditions similar to the experiment, the simulation [17] shows that the double peak distribution in Fig. 2 is a signature of saturation in the radiator undulator. In addition, with the CO₂ laser on, the center of mass of the beam in Fig. 2 shifts to the right by $\Delta\gamma/\gamma = 0.167\%$. For a 120 amp,

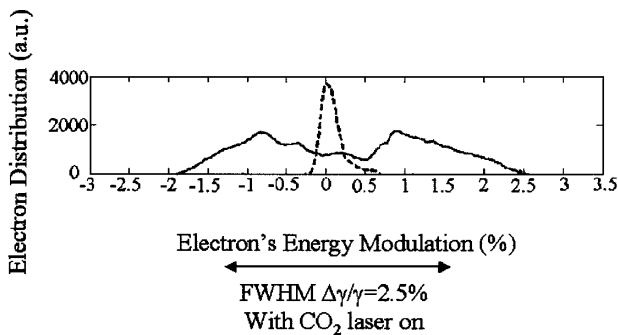


FIG. 2. The energy distribution of the electron beam after the electron spectrometer with (solid line) and without (dashed line) the CO₂ laser beam. The energy modulation is defined as the FWHM of the beam distribution. On the horizontal axis, positive values correspond to electron energy loss.

40 MeV electron beam this shift corresponds to 50 μ J of total energy loss, which is our typical measured HGHG output energy, consistent with the conservation of energy.

Further evidence of saturation is obtained by measuring the pulse energy of the second-harmonic (2.65 μ m) and the third-harmonic (1.77 μ m) components relative to the energy of the radiator fundamental (5.3 μ m). The fundamental and harmonic light were measured using an InSb detector with a calibrated spectral response. Comparable detector signal levels were produced using appropriate bandpass and neutral density filters. In Fig. 3, we plot the output energy (μ J) for the fundamental and first two harmonics versus electron beam energy modulation (%). As evident in the data [23–26] predict that the onset of an exponential increase in the harmonic energy at 2.65 and 1.77 μ m as the electron energy modulation approaches 2.5% is strong evidence of saturation. In Table I, the numerical results [26] and the experimental measurements of the ratio of the harmonic-to-fundamental energies are

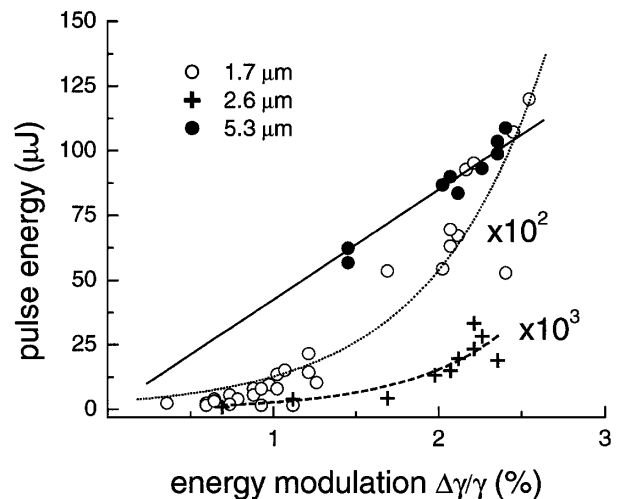


FIG. 3. Harmonic energy (μ J) versus electron beam energy modulation (%). The (●)'s are the data for the 5.3- μ m fundamental and the solid line is a linear fit. The energies for the second (+) and third (○) harmonics are multiplied by 10^3 and 10^2 , respectively. The second (dashed line) and third (dotted line) harmonic energy growth are fit by an exponential. Fits are constrained to a zero crossing.

TABLE I. The theoretical and experimentally measured harmonic-to-fundamental ratios.

Wavelength	Simulation	Experiment
2.65 μm	6×10^{-4}	2×10^{-4}
1.77 μm	1×10^{-2}	0.8×10^{-2}

presented for a 2.5% electron beam energy modulation. Good agreement is found between experiment and theory.

An important attribute of the HGHG approach as compared to SASE is the excellent longitudinal coherence of the output. A series of experiments were performed, aimed at characterizing the temporal output properties of the HGHG FEL. The duration of the intensity profile of the 5.3- μm HGHG pulse was studied using a standard Michelson design in a scanning, background-free, second-harmonic autocorrelator configuration. The small group velocity mismatch of the 1 mm thick AgGaSe₂ doubling crystal and geometric beam overlap in the crystal resulted in an instrumental resolution of better than 0.5 ps. The main sources of error in the measurement are imposed by the low-duty cycle of the CO₂ laser (0.05 Hz) and instabilities in the electron beam. In order to reduce scatter, each data point is a single shot measurement of the second harmonic signal normalized to the square of the fundamental energy. The normalized signal versus delay time (relative length difference between the two arms of the Michelson) is shown in Fig. 4. Assuming a Gaussian pulse shape, the duration is found to be $8.4/\sqrt{2} = 5.9 \pm 0.7$ ps. A transform limited Gaussian pulse [27] will produce a FWHM time-bandwidth ($\Delta f \Delta t$) product equal to $2 \ln 2/\pi$. In this experiment, the measured pulse duration and bandwidth of 15 nm yields a $\Delta f \Delta t$ product that is a factor of 2 larger

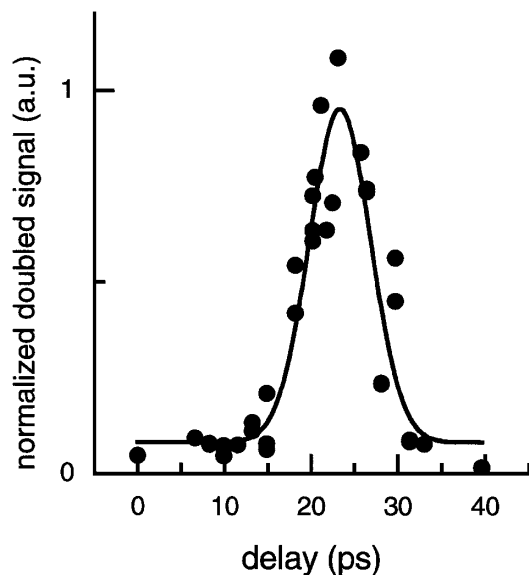


FIG. 4. The second-harmonic autocorrelation trace of the 5.3 μm HGHG output. The FWHM pulse width is $8.4/\sqrt{2} = 5.9 \pm 0.7$ ps as determined by a Gaussian fit.

than a Gaussian. More generally though, the value of the $\Delta f \Delta t$ product depends on the exact shape of the pulse; e.g., a flattop pulse gives a $\Delta f \Delta t \approx 0.9$. Clearly the limitations imposed by the scatter in the current experiment prohibits such a determination. However, short wavelength HGHG experiments planned at Brookhaven should result in a more complete optical characterization. Using the value of 5.9 ps for the HGHG output pulse and the measured energy of 100 μJ gives an output power of 17 MW, which is within a factor of 2 of the theoretical prediction [17] of 35 MW. Consistent with the earlier discussion, the simulation [17] also predicts deep saturation at this output power.

In another experiment, a Michelson interferometer was used to investigate the temporal coherence of the 5.3- μm HGHG output. The retroreflecting mirror in one arm of the interferometer was translated while the fringe visibility of the interference pattern was recorded on a thermal imaging camera. In order to collect more light we added a cylindrical mirror to produce a line-type image on the thermal camera. In an interferogram, the visibility [27] is defined as $(I_{\max} - I_{\min})/(I_{\max} + I_{\min})$ where I_{\max} and I_{\min} are the maximum and minimum average intensity, respectively, of the fringe pattern. The variation of fringe visibility as a function of delay, plotted in Fig. 5, is a measure of the coherence length of the pulse. The FWHM of the Gaussian fit in Fig. 5 yields a coherence time of 5.4 ± 0.5 ps.

The determination of the exact degree of longitudinal coherence is problematic since the correlation function [27] is dependent on the temporal profile, e.g., Gaussian, flattop, etc. Just like the autocorrelation measurement, fluctuations in the HGHG source predominantly introduced by instabilities in the electron beam and CO₂ laser severely limit the accuracy of the measurement and our ability to

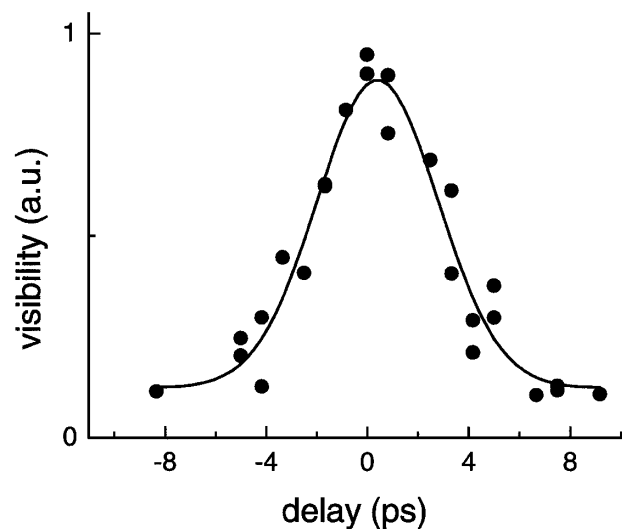


FIG. 5. The coherence length of the HGHG radiation pulse measured by plotting the fringe visibility as a function of delay. The solid curve is a Gaussian fit with a FWHM coherence time of 5.4 ± 0.5 ps.

discriminate line profiles. However, the agreement in the measured pulse duration and coherence time reveals that the HGHG pulse is temporally coherent across its intensity profile. This is further corroborated by the close agreement in the time-bandwidth product. Although our measurement is unable to determine the exact nature of the output pulse, it is clear that it has a high degree of longitudinal coherence.

In conclusion, we have characterized the energy and coherence properties of an HGHG FEL. The results demonstrate the utility of a HGHG FEL for producing intense coherent light pulses. Saturated FEL performance is confirmed by the extent of energy modulation introduced into the electron beam and the output energy of the harmonics and FEL fundamental light. Second harmonic autocorrelation, interferometry, and spectral measurements confirm that an HGHG FEL output is longitudinally coherent. The measurements are found to be consistent with theoretical simulations which can provide an important road map towards short wavelength operation. Work is currently underway at Brookhaven [28] for studying the HGHG process in the VUV (vacuum ultraviolet) spectral range. Furthermore, simulations show that the cascading of HGHG stages [29–32] can result in comparable hard x-ray production as a SASE FEL under similar operational parameters but with fully coherent output.

We thank all ATF personnel for their great help in making this experiment successful. This work was supported by U.S. Department of Energy, Office of Basic Energy Sciences, under Contracts No. DE-AC02-98CH10886 and No. W-31-109-ENG-38 and by Office of Naval Research Grant No. N00014-97-1-0845.

-
- [1] S. Leone, *Report of the BESAC Panel on Novel Coherent Light Sources* (U.S. Department of Energy, Washington, D.C., 1999).
- [2] The LCLS Design Study Group, Stanford Linear Accelerator Center (SLAC) Report No. SLAC-R-521, 1998.
- [3] Y. S. Debennev, A. M. Kondratenko, and E. L. Saldin, *Nucl. Instrum. Methods Phys. Res.* **193**, 415 (1982).
- [4] R. Bonifacio, C. Pellegrini, and L. Narducci, *Opt. Commun.* **50**, 373 (1984).
- [5] J. M. Wang and L. H. Yu, *Nucl. Instrum. Methods Phys. Res., Sect. A* **250**, 484 (1986).
- [6] K. J. Kim, *Nucl. Instrum. Methods Phys. Res., Sect. A* **250**, 396 (1986).
- [7] K. J. Kim, *Phys. Rev. Lett.* **57**, 1871 (1986).
- [8] S. Krinsky and L. H. Yu, *Phys. Rev. A* **35**, 3406 (1987).
- [9] L. H. Yu, S. Krinsky, and R. L. Gluckstern, *Phys. Rev. Lett.* **64**, 3011 (1990).
- [10] SASE gain of 10^5 at $12\ \mu\text{m}$ was reported in M. J. Hogan *et al.*, *Phys. Rev. Lett.* **81**, 4867 (1998).
- [11] SASE gain at 530 nm was observed at the LEUTL facility at APS/ANL; S. V. Milton *et al.*, *Phys. Rev. Lett.* **85**, 988 (2000).
- [12] SASE gain at 110 nm was observed at TTF/DESY; J. Andruszchow, *Phys. Rev. Lett.* **85**, 3825 (2000).
- [13] I. Ben-Zvi *et al.*, *Nucl. Instrum. Methods Phys. Res., Sect. A* **304**, 151 (1991).
- [14] L. H. Yu, *Phys. Rev. A* **44**, 5178 (1991).
- [15] L.-H. Yu *et al.*, *Nucl. Instrum. Methods Phys. Res., Sect. A* **445**, 301 (2000).
- [16] L.-H. Yu *et al.*, *Science* **289**, 932 (2000).
- [17] L.-H. Yu, in *Proceedings of the 1999 Particle Accelerator Conference, New York* (IEEE, Piscataway, NJ, 1999), p. 2474.
- [18] I. Boscolo and V. Stagno, *Nucl. Instrum. Methods Phys. Res.* **188**, 483 (1982).
- [19] I. Schnitzer and A. Gover, *Nucl. Instrum. Methods Phys. Res., Sect. A* **237**, 124 (1985).
- [20] R. Bonifacio *et al.*, *Nucl. Instrum. Methods Phys. Res., Sect. A* **296**, 787 (1990).
- [21] R. Prazeres *et al.*, *Nucl. Instrum. Methods Phys. Res., Sect. A* **304**, 72 (1991).
- [22] D. A. Jaroszynski *et al.*, *Nucl. Instrum. Methods Phys. Res., Sect. A* **375**, 456 (1996).
- [23] R. Bonifacio, L. De Salvo, and P. Pierini, *Nucl. Instrum. Methods Phys. Res., Sect. A* **293**, 627 (1990).
- [24] H. P. Freund, S. G. Biedron, and S. V. Milton, *IEEE J. Quantum Electron.* **36**, 275 (2000).
- [25] Zhirong Huang and Kwang-Je Kim, *Phys. Rev. E* **62**, 7295 (2000).
- [26] S. G. Biedron *et al.*, in *Proceedings of the 22nd International FEL Conference, Duke University, Durham, NC, 2000* (Ref. [25]).
- [27] L. Mandel and E. Wolf, *Optical Coherence and Quantum Optics* (Cambridge University Press, Cambridge, 1995), p. 166.
- [28] I. Ben-Zvi *et al.*, *Nucl. Instrum. Methods Phys. Res., Sect. A* **393**, II-10 (1997).
- [29] L. H. Yu and I. Ben-Zvi, *Nucl. Instrum. Methods Phys. Res., Sect. A* **393**, 96 (1997).
- [30] L. H. Yu and J. H. Wu, in *Proceedings of the ICFA Advanced Beam Dynamics Workshop on Future Light Sources*, edited by C. E. Eyberger (Argonne National Laboratory, Argonne, IL, 1999) [available at URL: <http://www.aps.anl.gov/conferences/FLSworkshop/proceedings/papers/wg1-01.pdf>].
- [31] J. H. Wu and L. H. Yu, in *Proceedings of the 22nd International FEL Conference, Duke University, Durham, NC, 2000* (Ref. [25]).
- [32] S. G. Biedron, S. V. Milton, and H. P. Freund, in *Proceedings of the 22nd International FEL Conference, Duke University, Durham, NC, 2000* (Ref. [25]).